

Quantum HodgeRank: Topology-Based Rank Aggregation on Quantum Computers

Caesnan M. G. Leditto,^{1,2,*} Angus Southwell,^{3,1} Behnam Tonekaboni,² Muhammad Usman,^{2,4,1} and Kavan Modi^{1,3,†}

¹*School of Physics and Astronomy, Monash University, Clayton, VIC 3168, Australia*

²*Quantum Systems, Data61, CSIRO, Clayton, VIC 3168, Australia*

³*Quantum for New South Wales, Haymarket, NSW 2000, Australia*

⁴*School of Physics, The University of Melbourne, Parkville, VIC 3052, Australia*

Rank aggregation techniques play a crucial role in identifying the best alternatives, but the inherent imbalance and incompleteness of real-world data pose significant challenges. The HodgeRank algorithm, which utilizes discrete exterior calculus on a graph, can overcome these issues and output a consistent global ranking of alternatives. Recently, higher-order networks have been employed to analyze complex multipartite interactions in network data. However, extending HodgeRank to ranking on higher-order networks requires computational costs that are exponential in the network dimension. To address this challenge, we develop a quantum algorithm that outputs a quantum state proportional to the HodgeRank solution. By incorporating quantum singular value transformation and tools from quantum topological data analysis, our approach achieves time complexity independent of the network dimension, avoiding the need for quantum random access memory or sparse access input models to create the boundary matrix in the higher dimensional discrete exterior calculus. We also present efficient algorithms and heuristics to extract meaningful information from the output quantum state, including an algorithm to compute the consistency of the ranking. Using our algorithm, the consistency measure estimation can potentially achieve superpolynomial quantum speedups for higher-order network data with specific structures. Beyond ranking tasks, our methods suggest that quantum computing could find fruitful applications in studying higher-order networks and discrete exterior calculus.

Introduction.—Ranking plays a crucial role in informed decision-making by comparing and contrasting different alternatives. Google’s PageRank [1, 2] and Netflix’s recommendation system [3] are both, at their core, ranking algorithms. Such ranking systems typically operate in environments where the data is noisy or incomplete. For instance, consider the task of ranking football teams based on their match results in a given season: here, the available data compares the teams pairwise, but some pairs may be missing, and thus the data is *incomplete*. Such ranking data appears commonly in systems with many alternatives, as many pairs might not have been explicitly compared.

The HodgeRank algorithm [4] overcomes such limitations by utilizing discrete exterior calculus [5, 6] to aggregate incomplete data – e.g., the pairwise match results – to derive a global ranking. It also provides a consistency measure for its ranking, indicating whether the data implies a strong consensus ranking of the alternatives or whether the data contains *ranking inconsistencies*, such as Condorcet paradoxes (rock-paper-scissors scenarios). HodgeRank generalizes PageRank and has applications in recommendation systems, social choice theory, arbitrage-free market detection, sports tournament ranking, online video quality assessments, market analysis, and protein folding analysis [4, 7–11].

The above examples mainly focus on ranking based on pairwise comparisons. Nevertheless, HodgeRank be-

longs to the toolkit of discrete exterior calculus on simplicial complexes, which can be generalised to higher-order networks [12–16] to model complex phenomena such as biological networks [17, 18] and chaotic Hamiltonian dynamics [19, 20], and has further applications to machine learning [21–23]. However, higher-dimensional HodgeRank (k -HodgeRank, for dimension k) computations are expensive: the complexity scales exponentially in the network dimension, which hinders the practical applications and exploration of higher-order network models despite strong evidence for their importance in many real-world systems [24–26].

In this Letter, we propose a quantum algorithm that prepares a quantum state proportional to the output of the k -HodgeRank algorithm that is exponentially faster in k than generalizations of standard classical methods (and polynomially faster for $k = 1$ which corresponds to pairwise preference data). This advantage may be reduced in the readout process, i.e., acquiring classical information via quantum state tomography. However, the scaling advantage is maintained when extracting answers to specific questions, modulo some caveats we discuss later. We give algorithms for three applications to (i) measure the rankability of the data, (ii) relatively rank a set of chosen alternatives, and (iii) return top-ranking alternatives. In particular, the first application might achieve a superpolynomial advantage, similar to other quantum algorithms that estimate the fit quality of data [27, 28], while the latter applications are more heuristic and data-dependent. We highlight that, while we focus on ranking algorithms here, the tools developed in the Letter will have natural applications to other

* caesnan.leditto@monash.edu

† kavan.modi@monash.edu

aspects of higher-dimensional discrete exterior calculus, such as solving general least square [29] and boundary value problems [30, 31].

HodgeRank.— We briefly describe HodgeRank and the associated mathematical problems (see [4] for details). HodgeRank provides a global ranking of alternatives $\mathcal{V} := \{v_1, \dots, v_n\}$. The input to HodgeRank is the aggregated pairwise preferences of voters, modelled by an edge flow $\mathbf{s}^1 : \mathcal{E} \rightarrow \mathcal{R}$ on a comparison graph $\mathcal{G} = (\mathcal{V}, \mathcal{E})$, which can be viewed as a vector $\mathbf{s}^1 \in \mathbb{R}^{|\mathcal{E}|}$ by (arbitrarily) orienting each edge in the edge set \mathcal{E} . The graph \mathcal{G} need not be complete, as not all pairs of alternatives need to be compared directly. The value $\mathbf{s}^1([v_i, v_j])$ represents the preference for alternative i over j , where $[\cdot, \cdot]$ denotes that the edge is oriented.

Given a comparison graph \mathcal{G} and preference data \mathbf{s}^1 , the pairwise ranking problem can then be formulated as a weighted ℓ_2 minimization problem with solution

$$\mathbf{s}_G^1 = \arg \min_{\mathbf{x} \in \text{im}(\mathbf{B}_1^\dagger)} \left[\sum_{1 \leq i < j \leq n} w_{ij} (x_{ij} - \mathbf{s}^1([v_i, v_j]))^2 \right], \quad (1)$$

where w_{ij} represents the weight associated to the data on (oriented) edge $[v_i, v_j]$ and \mathbf{B}_k is a matrix representation of the k -th boundary operator of a clique complex $\mathcal{K}_n(\mathcal{G})$ (see Appendix I). The space $\text{im}(\mathbf{B}_1^\dagger)$ contains so-called *conservative* edge flows, which means there exists $\mathbf{s}_*^0 \in \mathbb{R}^{|\mathcal{V}|}$ such that $\mathbf{s}_G^1([v_i, v_j]) = \mathbf{s}_*^0(v_i) - \mathbf{s}_*^0(v_j)$. In a discrete exterior calculus sense, \mathbf{s}_G^1 is an analogue of the gradient of the *potential function* \mathbf{s}_*^0 .

HodgeRank then computes the potential (or score) function \mathbf{s}_*^0 from Eq. (1) by $\mathbf{B}_1^\dagger \mathbf{s}_*^0 = \mathbf{s}_G^1$. The vector \mathbf{s}_*^1 defines a global ranking of the alternatives: the score HodgeRank gives to alternative v_i is $\mathbf{s}_*^0(v_i)$, and $v_i \succeq v_j$ whenever $\mathbf{s}^0(v_i) \geq \mathbf{s}^0(v_j)$. In this Letter, we set $w_{ij} = 0$ if v_i, v_j are not compared, and 1 otherwise; we discuss this assumption in Appendix III. Under this assumption, the score function \mathbf{s}_*^0 is given by $\mathbf{s}_*^0 = (\mathbf{B}_1 \mathbf{B}_1^\dagger)^+ \mathbf{B}_1 \mathbf{s}^1$, where $+$ denotes the Moore-Penrose pseudoinverse. The most positive elements of \mathbf{s}_*^0 correspond to the best alternatives. The length of the vector \mathbf{s}_G^1 , relative to the length of \mathbf{s}^1 , is a measure of the rankability of the alternatives according to the data \mathbf{s}^1 .

In higher dimensions, k -HodgeRank generalizes the comparison graph to a clique complex $\mathcal{K}_n(\mathcal{G})$ of dimension k , defined on the same vertex set \mathcal{V} . Instead of $\mathbf{s}^1 \in \mathbb{R}^{|\mathcal{E}|}$ assigning a real number to each edge (or 1-simplex), the data vector $\mathbf{s}^k \in \mathbb{R}^{n_k}$ assigns a real number s_k^i to each k -simplex σ_k^i (a $(k+1)$ -element subset of \mathcal{V}), where $i \in [n_k] := \{0, \dots, n_k - 1\}$ and n_k is the number of k -simplices in $\mathcal{K}_n(\mathcal{G})$. Define \mathbf{s}_*^{k-1} as the solution to k -HodgeRank, the higher-dimensional analogue of Eq. (1), that is

$$\mathbf{s}_*^{k-1} = \left(\mathbf{B}_k \mathbf{B}_k^\dagger \right)^+ \mathbf{B}_k \mathbf{s}^k. \quad (2)$$

This vector assigns a score to each $(k-1)$ -simplex in $\mathcal{K}_n(\mathcal{G})$. Similarly, one may define $\mathbf{s}_G^k := \mathbf{B}_k^\dagger \mathbf{s}_*^{k-1}$, which

is a projection of \mathbf{s}^k onto the space of conservative edge flows on the k -simplices of $\mathcal{K}_n(\mathcal{G})$. We define the k -HodgeRank problem as finding \mathbf{s}_*^{k-1} given the following (classically stored) information: (i) the vector \mathbf{s}^k , (ii) a matching list of k -simplices $\{\sigma_k^i\}_i$ and $(k-1)$ -simplices $\{\sigma_{k-1}^j\}_j$, (iii) the adjacency matrix of the graph underlying the clique complex.

Quantum least squares algorithms.—The HodgeRank problem in Eq. (1) is a specific type of weighted least squares problem. For $k=1$, this problem can be solved via an exact classical computation with complexity $O(n^3)$ [4]. Approximate algorithms, such as various graph Laplacian solvers [32–34] or topological signal processing (TSP) methods [10, 21], have complexities that scale roughly quadratically in n , with varying dependence on the approximation parameters. In higher dimensions, computing \mathbf{s}_G^k and \mathbf{s}_*^{k-1} via least squares using classical sparse linear equation solvers has worst-case scaling $\Omega(n_k)$ [29, 35], where n_k is the number of k simplices. This follows from the fact that \mathbf{B}_k is an $n_k \times n_{k-1}$ matrix with $(k+1)n_k$ non-zero entries. Generalizing the TSP approach to avoid matrix multiplication by instead performing repeated matrix-vector multiplication similarly leads to (approximate) algorithms with complexity $\Omega(n_k)$. This is problematic because the number of k -simplices can be as large as $\binom{n}{k+1}$, which is asymptotically $\frac{n^{k+1}}{(k+1)!}$ when $k = o(\sqrt{n})$. This shows that the dimension of the simplices considered is the crucial factor in the complexity of solving the k -HodgeRank problem.

Quantum computers can potentially speed up certain high-dimensional linear algebra computations. In recent years, there have been several quantum algorithms proposed for tackling least square problems [27, 28, 36–38]. The best known quantum least squares algorithm requires approximately $\tilde{O}(\alpha_{\mathbf{A}} \kappa_{\mathbf{A}} \log(1/\varepsilon))$ calls to a block encoding of \mathbf{A} , where $\alpha_{\mathbf{A}}$ is the scaling factor coming from implementing the block encoding of the matrix \mathbf{A} , $\kappa_{\mathbf{A}}$ is the effective condition number, and ε is the accuracy parameter [38]. Their algorithm combines QSVT and variable-time amplitude amplification (VTAA) [39], modifying the previous approach given by Ref. [36].

However, this algorithm and the other previously mentioned quantum least squares algorithms are of limited use for solving k -HodgeRank. Block encodings of the boundary operator \mathbf{B}_k constructed via quantum random access memory (QRAM) or a sparse access input model (SAIM) suffer from poor worst-case scaling due to $\alpha_{\mathbf{B}_k}$ scaling with either the Frobenius norm or the sparsity of \mathbf{B}_k [36, 38], which both have worst-case scaling $\Omega(n_k)$ as discussed previously. On the other hand, there are no currently known methods for block encoding boundary operators that do not rely on such input models. We summarize these relationships between classical least squares algorithms, quantum least squares algorithms, HodgeRank, and quantum k -HodgeRank in Figure 1 in Appendix III.

In the next section, we develop a quantum algorithm

to solve k -HodgeRank on a quantum computer. Given a quantum state that encodes simplicial signal values and a (classically stored) list of edges in the clique complex, our algorithm outputs a quantum state that approximates a state proportional to Eq. (2). Its complexity has quadratically worse dependence on the effective condition number than Ref. [38], but a much simpler implementation and applicability to projected unitary encodings (PUEs). Moreover, the scaling factors present in the PUEs of \mathbf{B}_k and \mathbf{B}_{k+1} are only \sqrt{n} [40] or n [41] depending on the implementation method, which is much smaller than the potentially exponential scaling factors that can arise from using QRAM/SAIM. We do not claim that our method is optimal — indeed, it is possible that the algorithm presented in Ref. [38] could also be adapted to work for projected unitary encodings while maintaining the improved dependence on the effective condition number. Rather than optimizing the method, we combine well-known quantum algorithm tools from quantum topological data analysis with the quantum singular value transformation to solve a classically studied class of least squares problems without appealing to QRAM or SAIM to encode the desired matrices. *Quantum HodgeRank.*— We now give a quantum algorithm for k -HodgeRank that scales exponentially better than its classical counterparts in k . Our algorithm, which we call quantum (k -)HodgeRank, prepares a quantum state that encodes an approximate solution to Eq. (2), with a circuit depth that does not, in general, depend on the dimension k . Here, we define our computational model as a classical control procedure running quantum algorithm subroutines.

We build quantum k -HodgeRank on the recently developed quantum algorithm for topological signal processing (QTSP) [42] for analyzing higher-order networks [12–16, 19]. We assume that there is a quantum state preparation unitary \mathbf{U}_{prep} that takes classical data \mathbf{s}^k and prepares the state

$$|\mathbf{s}^k\rangle := \frac{1}{\|\mathbf{s}^k\|_2} \sum_{i \in [n_k]} s_i^k |\sigma_k^i\rangle, \quad (3)$$

where $|\sigma_k^i\rangle$ is n -qubit computational basis state representing σ_k^i defined in [41, 43] (given in Eq. (18) in Appendix II). We discuss the complexities of our applications in terms of the number of calls to \mathbf{U}_{prep} .

The QTSP algorithm combines the quantum singular value transformation (QSVT) [44, 45] and the projected unitary encodings $\mathbf{U}_{\mathbf{B}_k}$ and $\mathbf{U}_{\mathbf{B}_{k+1}}$ of the boundary matrices \mathbf{B}_k and \mathbf{B}_{k+1} [40, 46] (described in Appendix II). It prepares, upon successful postselection in the ancilla (which occurs with probability approximately $\mathcal{N}^2 := \|\mathbf{H}(\mathbf{B}_k/\sqrt{n}, \mathbf{B}_{k+1}^\dagger/\sqrt{n})|\mathbf{s}^k\rangle\|_2^2$), the *filtered* state

$$|\mathbf{s}_{\text{fil}}^k\rangle := \frac{1}{\mathcal{N}} H\left(\frac{\mathbf{B}_k}{\sqrt{n}}, \frac{\mathbf{B}_{k+1}^\dagger}{\sqrt{n}}\right) |\mathbf{s}^k\rangle. \quad (4)$$

Here $H(x, y) : [-1, 1]^2 \rightarrow [-1, 1]$ is a sum of two real polynomials $p(x)$ and $q(y)$ respectively, each with degree

at most D , applied to the singular values of the respective matrices. The polynomial $H(x, y)$ is chosen so that $|\mathbf{s}_{\text{fil}}^k\rangle$ extracts specific information about the higher-order network data. In classical topological signal processing, p and q are usually either both even or one is zero. The QTSP algorithm requires one call to \mathbf{U}_{prep} as well as $O(D)$ calls to $\mathbf{U}_{\mathbf{B}_k}$, $\mathbf{U}_{\mathbf{B}_{k+1}}$, their inverses, and $O(D)$ applications of \mathbf{C}_{Π_j} NOT for $j \in \{k-1, k, k+1\}$, where Π_j is the projector onto the states corresponding to k -simplices [47, 48], as well as post-selection on the correct ancilla state (see Appendix II for more details). The classical control is used to implement the \mathbf{C}_{Π_j} NOT gates, as the structure of their circuit depends on the edges in the underlying graph \mathcal{G} of the clique complex $\mathcal{K}_n(\mathcal{G})$. The quantum circuit for QTSP has non-Clifford gate depth $O(Dn \log n)$ and uses $O(n)$ qubits. We review the general QTSP algorithm and its complexity in Appendix II (see [42] for further details).

We now derive quantum k -HodgeRank by utilizing QTSP to output a quantum state $|\tilde{\mathbf{s}}_*^{k-1}\rangle$ that approximates

$$|\mathbf{s}_*^{k-1}\rangle := \frac{1}{\mathcal{N}_*} \sum_{i \in [n_{k-1}]} s_{i,*}^{k-1} |\sigma_{k-1}^i\rangle \quad (5)$$

where $\mathcal{N}_* := \|(\mathbf{B}_k \mathbf{B}_k^\dagger)^+ \mathbf{B}_k |\mathbf{s}^k\rangle\|_2$. To obtain a state approximating $|\mathbf{s}_*^{k-1}\rangle$, we start with the state $|\mathbf{s}^k\rangle$ as in Eq. (3). Then using QTSP, we apply an approximation of $(\mathbf{B}_k \mathbf{B}_k^\dagger)^+ \mathbf{B}_k$, given by a polynomial $H(\mathbf{B}_k/\sqrt{n}, \mathbf{B}_{k+1}^\dagger/\sqrt{n}) = p(\mathbf{B}_k/\sqrt{n})$ solely in \mathbf{B}_k , to the input state. The polynomial $H(x, y)$ is defined by $q(y) = 0$ and $p(x) = x g_\varepsilon(x^2)$, where $g_\varepsilon(x)$ is $(\varepsilon/(2\kappa_k^2))$ -close to $1/(2\kappa_k^2 x)$ on the domain $[-1, -1/\kappa_k^2] \cup [1/\kappa_k^2, 1]$ (see [44, 49] for details). Here, κ_k is the effective condition number of \mathbf{B}_k (the ratio of the largest and smallest nonzero singular values) and $\varepsilon \in (0, 1/2)$. Importantly, $g_\varepsilon(x)$ is a polynomial of degree $O(\kappa_k^2 \log(\sqrt{n}\kappa_k/\varepsilon))$, and

$$\left\| \left(\mathbf{B}_k \mathbf{B}_k^\dagger \right)^+ \mathbf{B}_k - \frac{2\kappa_k^2}{\sqrt{n}} p\left(\frac{\mathbf{B}_k}{\sqrt{n}}\right) \right\|_2 \leq \varepsilon. \quad (6)$$

The output of the above protocol, after successful post-selection on the ancilla (which occurs with probability $\Omega(n\tilde{\mathcal{N}}_*/(4\kappa_k^4))$, where $\tilde{\mathcal{N}}_* := \|\mathbf{H}(\mathbf{B}_k/\sqrt{n})|\mathbf{s}^k\rangle\|_2$), is

$$|\tilde{\mathbf{s}}_*^{k-1}\rangle := \frac{\sqrt{n}}{2\kappa_k^2 \tilde{\mathcal{N}}_*} \sum_{i \in [n_{k-1}]} \tilde{s}_{i,*}^{k-1} |\sigma_{k-1}^i\rangle, \quad (7)$$

which is a $2\varepsilon/(\mathcal{N}_* - \varepsilon)$ -approximation to $|\mathbf{s}_*^{k-1}\rangle$ (in ℓ_2 norm) if $\mathcal{N}_* > \varepsilon$. As we discuss further in Appendix III, in cases where \mathbf{s}^k has high rankability (defined formally in Application 1), ε can be chosen such that $|\tilde{\mathbf{s}}_*^{k-1}\rangle$ is a $4\varepsilon/\mathcal{N}_*$ -approximation to $|\mathbf{s}_*^{k-1}\rangle$, making the output a good approximation without significantly affecting the complexity. It follows from the complexity of QTSP

that the algorithm to prepare $|\tilde{\mathbf{s}}_*^{k-1}\rangle$ from $|\mathbf{s}^k\rangle$, excluding post-selection, uses $O(n)$ qubits and has non-Clifford gate depth

$$O(n\kappa_k^2 \log(n) \log(\sqrt{n}\kappa_k^2/\varepsilon)). \quad (8)$$

If κ_k is small (e.g. not growing exponentially in k), this is much more efficient than the exact classical computation of $\tilde{\mathbf{s}}_*^{k-1}$, even when k is a small constant. Notable examples of simplicial complexes with slowly-growing (or even constant in k) effective condition numbers are given in [41]. Analogously computing $p(\mathbf{B}_k)\mathbf{s}^k$ on a classical computer requires $\tilde{O}(\kappa_k^2)$ iterations of matrix-vector multiplication that each require $O(n_k)$ operations [50]. This again highlights the dependency of the simplex dimension in the classical complexity, particularly for complexes with many k -simplices, since $n_k = \Theta\left(\binom{n}{k+1}\right) \approx \Theta(n^{k+1})$ is possible.

Similar to other quantum algorithms for linear algebra tasks, such as [36, 51], the speedup of our algorithm comes from preparing the k -HodgeRank solution as a quantum state. Extracting a full classical representation of $|\tilde{\mathbf{s}}_*^{k-1}\rangle$ is generally expensive. We present some applications that recover relevant information while avoiding full-state tomography where possible. These applications use quantum k -HodgeRank (or a straightforward modification) as a subroutine, and their complexities do not in general depend on k . This indicates that quantum k -HodgeRank, and QTSP in general, can potentially speed up specific computations defined on high-dimensional simplicial complexes. In the following applications, we assume that the effective condition numbers κ_k and κ_{k+1} of \mathbf{B}_k and \mathbf{B}_{k+1} , respectively, are known and (ideally) small.

Approximating consistency measures.—We provide algorithms to measure the rankability of data in terms of so-called consistency and local inconsistency measures $R(k) \in [0, 1]$ and $R_C(k) \in [0, 1]$, generalising definitions from [4]. The consistency measure associated to the data \mathbf{s}^k is the (Euclidean) length of \mathbf{s}_G^k relative to \mathbf{s}^k . This can be viewed as a measure of “goodness of fit” in a least squares sense. Similarly, the local inconsistency measure is the relative length of the projection of \mathbf{s}^k onto $\text{im}(\mathbf{B}_{k+1})$, which we denote \mathbf{s}_C^k . Explicitly,

$$R(k) := \left(\frac{\mathbf{s}_G^k \cdot \mathbf{s}^k}{\|\mathbf{s}^k\|^2}\right)^{1/2} \quad \text{and} \quad R_C(k) := \left(\frac{\mathbf{s}_C^k \cdot \mathbf{s}^k}{\|\mathbf{s}^k\|^2}\right)^{1/2}. \quad (9)$$

The value $R(k)$ measures whether the (sets of) alternatives are globally ranked in a meaningful way based on the data, where larger values indicate high rankability. Conversely, $R_C(k)$ measures the presence of non-transitive preference relationships in the data, that is, cases where the consensus prefers A over B , B over C , and yet C over A . This has applications in finding arbitrage in currency exchange markets [4]. These measures are related to what is known as the Hodge decomposition (see Appendix I for a brief introduction to the underlying topology).

We provide algorithms to compute ε -approximations to $R(k)$ and $R_C(k)$ (see Appendix IV for more details). It follows from Eq. (9) that $R(k) = (\langle \mathbf{s}^k | \Pi_G | \mathbf{s}^k \rangle)^{1/2}$, where $\Pi_G := \mathbf{B}_k^\dagger (\mathbf{B}_k \mathbf{B}_k^\dagger)^+ \mathbf{B}_k$ is the projector onto $\text{im}(\mathbf{B}_k^\dagger)$. Thus, we can approximate $R(k)$ using a Hadamard test, which can be accelerated further with amplitude estimation [52], provided we can make an approximate PUE of the projector Π_G . We do this using QTSP by setting $H(x, y) = p(x) = x^2 g_{\varepsilon^2/2}(x^2)$, where as before g_ε is a polynomial which $\varepsilon/(2\kappa_k^2)$ -approximates $1/(2\kappa_k^2 x)$. It follows that $\|\Pi_G - 2\kappa_k^2 p(\mathbf{B}_k/\sqrt{n})\|_2 \leq \varepsilon^2/2$, where $p(x)$ is degree $D = O(\kappa_k^2 \log(n\kappa_k^2/\varepsilon^2))$ (see Theorem 2 in [42]). Thus, if $\mathbf{U}_{\Pi_G} = \text{QTSP}(k, \mathcal{K}_n, x^2 g_{\varepsilon^2/2}(x^2))$ is the unitary that block encodes $p(\mathbf{B}_k/\sqrt{n})$ in the subspace defined by the ancilla in state $|0\rangle^{\otimes a}$, then

$$2\kappa_k^2 \langle \mathbf{s}^k | \langle 0 |^{\otimes a} \mathbf{U}_{\Pi_G} | \mathbf{s}^k \rangle | 0 \rangle^{\otimes a} = (R(k))^2 \pm \varepsilon^2/2. \quad (10)$$

The value of $R(k)$ can be ε -approximated with success probability $1 - \delta$ using $O(\kappa_k^2 \log(1/\delta)/\varepsilon^2)$ controlled applications of \mathbf{U}_{prep} and $\text{QTSP}(k, \mathcal{K}_n, x^2 g_{\varepsilon^2/2}(x))$. Thus, if \mathbf{U}_{prep} has non-Clifford gate depth G , the overall non-Clifford gate depth of this procedure is $O\left(\kappa_k^2 \varepsilon^{-2} \log(1/\delta) \left(G + n\kappa_k^2 \log n \log\left(\frac{n\kappa_k^2}{\varepsilon^2}\right)\right)\right) \approx \tilde{O}\left(\kappa_k^2 \varepsilon^{-2} \log(1/\delta) (G + n\kappa_k^2)\right)$, where \tilde{O} hides logarithmic factors of n , ε , and κ_k . In the $k = 1$ case, this algorithm achieves a polynomial speed-up over the exact classical algorithm, which runs in time $O(n^3)$ [4], provided G is small. The total runtime of the analogous approximate computation via classical topological signal processing (TSP) [21, 23] is $O(nkn_k\kappa_k^2 \log(n\kappa_k^2/\varepsilon^2))$ [10, 50]. As discussed earlier, the linear dependence on n_k leads to exponential (in k) worst-case scaling.

This application can serve as a quantum-accelerated litmus test to check whether performing k -HodgeRank classically is worthwhile without the large classical computing time required to determine $R(k)$ exactly. An approximation of $R(k)$ up to a small constant, e.g. $\varepsilon \approx 0.1$, would be indicative of whether the underlying data \mathbf{s}^k is amenable to a global ranking via k -HodgeRank.

Computing the local inconsistency measure is similar. In this task we estimate $R_C(k) = (\langle \mathbf{s}^k | \Pi_C | \mathbf{s}^k \rangle)^{1/2}$, where Π_C is the projector onto $\text{im}(\mathbf{B}_{k+1})$. Thus, instead of applying $p(x)$ as defined above, apply a filter $H(x, y) = q(y) = y^2 g_{\varepsilon^2/2}(y^2)$ such that $2\kappa_{k+1}^2 q(\mathbf{B}_{k+1}^\dagger/\sqrt{n})$ is $(\varepsilon^2/2)$ -close to the projector Π_C in spectral norm. Analogously to approximating the consistency score, one can use an accelerated Hadamard test that computes a ε -approximation to $R_C(k)$ with a probability of success $1 - \delta$ using $\tilde{O}(\kappa_{k+1}^2 \varepsilon^{-2} \log(1/\delta))$ applications of \mathbf{U}_{prep} and $\text{QTSP}(k, \mathcal{K}_n, y^2 g_{\varepsilon^2/2}(y^2))$. The exact classical computation for this quantity, as given by Jiang et al. [4], is $O(n^9)$ in the $k = 1$ case. Implementing this same matrix polynomial via classical TSP methods has complexity $O(nkn_{k+1}\kappa_{k+1}^2 \log(n\kappa_{k+1}^2/\varepsilon^2))$ for general k , and has the same exponential scaling pitfalls as computing

$R(k)$ classically.

Relative rankings of few alternatives.—We combine quantum k -HodgeRank and amplitude estimation to approximate the scores of individual alternatives. This gives a heuristic way of relatively ranking a small set of alternatives without full-state tomography or performing the full classical computation. We give the basic description here, for more details on this application see Appendix V.

Let \mathbf{U}_{k-1}^i be a unitary with action $\mathbf{U}_{k-1}^i |0\rangle = |\sigma_{k-1}^i\rangle$, which is simply a tensor product of X gates on the appropriate qubits. By calling controlled applications of quantum k -HodgeRank and state preparation unitaries \mathbf{U}_{prep} and \mathbf{U}_{k-1}^i , we can implement the Hadamard test to approximate the score $s_{*,i}^{k-1}$ of each $(k-1)$ -simplex σ_{k-1}^i . Approximating the scores for a set of L alternatives up to an additive error ε requires $O(n)$ qubits and $O(L\kappa_k^2 \log(L/\delta)/(\sqrt{n}\varepsilon))$ calls to each of $\text{QTSP}(k, \mathcal{K}_n, xg_{\varepsilon/2}(x))$, \mathbf{U}_{prep} , and \mathbf{U}_{k-1}^i . Excluding the complexity of the state preparation unitary \mathbf{U}_{prep} , the total non-Clifford gate depth is $\tilde{O}(L\kappa_k^4 \sqrt{n} \log(L/\delta)/\varepsilon)$. One can relatively rank L alternatives $\sigma_{k-1}^{i_1}, \dots, \sigma_{k-1}^{i_L} \in \mathcal{K}_n(\mathcal{G})$ by approximating each of their scores and ranking them according to these approximations.

For small L (e.g. $L = o(\sqrt{n})$), this procedure is, in principle, more efficient than computing HodgeRank classically. However, this procedure is heuristic because an appropriate value for ε is not obvious a priori, and there may be data where $\varepsilon = O(n^{-ck})$ is needed to extract useful information. For example, as k grows, the number of k -simplices may grow exponentially. Thus, the average amplitude of a basis state in $|\mathbf{s}^{k-1}\rangle$ might vanish exponentially in k (since the quantum state has unit norm). As a result, the accuracy and precision requirements of both $xg_{\varepsilon/2}(x^2)$ and the Hadamard test may need to scale exponentially with k to extract meaningful information from the approximate amplitudes. This would limit the general advantage gained over classical methods to polynomial scaling at best. However, there may be specific choices of clique complex $\mathcal{K}_n(\mathcal{G})$ and \mathbf{s}^k data where the quantum advantage is greater.

Finding good alternatives.— We now consider the problem of determining an approximate score for every $(k-1)$ -simplex. As mentioned previously, full-state tomography can be very expensive. However, one can use tomography techniques given in [53] to obtain a classically stored vector $\hat{\mathbf{s}}_*^{k-1}$ which is an ℓ_∞ norm approximation to $|\mathbf{s}_*^{k-1}\rangle$. As detailed in Appendix VI, one can determine the score of every $(k-1)$ -simplex, up to additive error $O(\varepsilon)$, in $O(\kappa_k^4 n \varepsilon^{-2})$ applications of $\text{QTSP}(k, \mathcal{K}_n, xg_\varepsilon(x))$ and \mathbf{U}_{prep} .

One can use this to find an alternative that has a score within additive error $O(\varepsilon)$ of the best alternative, which for an appropriate choice of ε will correspond to a high-ranking alternative. This ℓ_∞ norm approximation can also be used to determine whether the alternatives can be

classified into subsets with similar scores within subsets and large differences in scores between subsets. However, this method for returning good alternatives is at best heuristic, as an appropriate choice of ε cannot be easily determined from $|\mathbf{s}^k\rangle$, and indeed ε may need to be arbitrarily small to extract meaningful information (e.g. returning an alternative whose score is “close” to the best score), as the amplitudes of the state $|\mathbf{s}_*^{k-1}\rangle$ may be arbitrarily close.

Conclusions. — Quantum HodgeRank and the subsequent use cases presented here provide an alternative avenue for exploring quantum advantage using tools created for quantum topological data analysis (QTDA). This provides a promising path towards solving specific classes of least squares problems, with applications to ranking and discrete exterior calculus, without the issues arising from using QRAM/SAIM to encode the matrix. Standard techniques for dequantizing quantum linear algebra algorithms [54–56] more broadly, have not historically worked for QTDA due to the potentially exponential scaling of the Frobenius norm of the boundary operator. Dequantized QTDA algorithms [57] rely on the relationship to the problem of projecting to the null space of $\mathbf{B}_k^\dagger \mathbf{B}_k + \mathbf{B}_{k+1}^\dagger \mathbf{B}_{k+1}$ (known as the Hodge/combinatorial Laplacian [58]) and estimating its rank. HodgeRank and the applications considered here do not a priori share this connection to finding the rank of the null space, and so the methods used to dequantize QTDA do not obviously apply. An interesting future direction would be determining to what extent QTSP and quantum k -HodgeRank can be dequantized.

As HodgeRank offers an alternative solution to find the stationary distribution of the random walk on the web page graph [4], the quantum HodgeRank algorithm could be considered as a variant of quantum PageRank algorithms [59, 60]. We also note that while recommendation systems are related to rank aggregation problems, the problem formulation and methods used in HodgeRank differ significantly from those studied by Kerenidis and Prakash [37]. This distinction extends to the underlying quantum algorithms as well.

We note that in this Letter we often compare approximate quantum algorithms to exact classical methods or deterministic methods described using stock-standard matrix multiplication, inversion, and diagonalization subroutines. Comparing to a broader range of classical algorithms would be a natural next step. While other approximate methods for computing \mathbf{s}_*^{k-1} as given in Eq. (2) do exist for $k=1$ and some limited cases for $k=2$ [29, 34, 35], these methods do not naturally extend to general Laplacian linear equation solvers for $k \geq 2$. In general, Laplacian equations with $k=2$ are as difficult to solve as general linear equations [29], where sparse approximate solvers for linear equations with N nonzero coefficients and condition number κ run in time $O(\min\{N^{2.27159}, N\kappa\})$ [29]. In the case of Laplacian equations for larger k , $N = n_k$ and thus can grow exponentially in k , as each k -simplex may be adjacent to

$\Omega(nk)$ other k -simplices. This suggests, at least intuitively, that Laplacian equations for general k are expected to be hard to solve, even approximately.

We highlight the method used in [29] that maps general linear equations to linear equations in a boundary matrix of a simplicial complex of dimension $k = 2$. This mapping allows any least square problem to be realized as a least square problem where the matrix is a boundary matrix \mathbf{B}_2 of a simplicial complex. As such, one could theoretically use quantum 2-HodgeRank to solve general linear equations. In practice, the complexity of performing the mapping itself scales linearly in the number of variables, so this would not provide more than a polynomial advantage at best. However, with this in mind, it is possible that quantum k -HodgeRank could be used to solve more general least square problems. In particular, if the mapping used in [29] to map general linear equations to linear equations of boundary matrices of arbitrary dimension in a more vertex-compact form, this could provide an alternative avenue for new quantum linear system solvers. A simpler intermediate step to broadening the use cases of our methods would be to characterize the boundary matrices of simplicial (or clique) complexes. For example, if \mathbf{B} is a boundary matrix of a simplicial complex, all entries of \mathbf{B} must be in $\{-1, 0, +1\}$, and each column must have exactly $k + 1$ nonzero entries. A complete characterization of these matrices would allow us to determine the class of least squares problems for which quantum k -HodgeRank could offer a speed-up compared to classical algorithms or QRAM/SAIM-based quantum methods.

In the framework of discrete exterior calculus [5, 6],

quantum k -HodgeRank, and more broadly QTSP, could potentially have applications in studying the Kuramoto model of coupled oscillators [61] and its higher-order analogues [19, 20]. Moreover, discretized and triangulated domains are types of higher-order networks. Hence, the algorithm could be applied to such domains to solve variants of boundary value problems in fluid dynamics [62–64] and plasma physics [65, 66].

Since our algorithm relies on fast methods to prepare the initial state $|s^k\rangle$, applications with quantum data would be desirable. One possible avenue is measuring quantum contextuality [67, 68], as sheaves can be defined over simplicial complexes. We also anticipate that the quantum k -HodgeRank, and more broadly QTSP, could potentially have applications in studying multipartite interactions in complex quantum networks [69].

On the more mathematical side, Jiang et al. [4] note that the mathematical tools apply for higher-order networks modelled by simplicial complexes as well, as the definition and relevant properties of the boundary operators \mathbf{B}_k hold for arbitrary k . Nevertheless, they do not give an operational meaning to the higher-dimensional analogues. Finding an operational interpretation for k -HodgeRank could have wide-reaching applications to higher-order network modelling. It would provide more concrete applications where these quantum algorithms perform best.

ACKNOWLEDGEMENTS

We thank Pedro C. S. Costa for several technical discussions. C.M.G.L. is supported by a Monash Graduate Scholarship and CSIRO Data 61 Top-Up Scholarship.

-
- [1] S. Brin and L. Page. *Computer Networks*, 30:107–117, 1998.
 - [2] *Google’s PageRank and Beyond: The Science of Search Engine Rankings*. Princeton University Press, Princeton, 2006.
 - [3] C. A. Gomez-Uribe and N. Hunt. *ACM Trans. Manage. Inf. Syst.*, 6(4), dec 2016.
 - [4] X. Jiang, L. H. Lim, Y. Yao, and Y. Ye. *Mathematical Programming*, 127(1):203–244, 2011.
 - [5] A. N. Hirani. Phd thesis, Caltech, California, USA, June 2014.
 - [6] M. Desbrun, E. Kanso, and Y. Tong. In *ACM SIGGRAPH 2006 Courses, SIGGRAPH ’06*, page 39–54, New York, NY, USA, 2006. Association for Computing Machinery.
 - [7] Q. Xu, Q. Huang, T. Jiang, B. Yan, W. Lin, and Y. Yao. *IEEE Transactions on Multimedia*, 14(3):844–857, 2012.
 - [8] R. K. Sizemore, June 2014.
 - [9] T. Do, T. Nguyen, and H. Pham. In *Proceedings of the 1st International Electronics Communication Conference, IECC ’19*, page 90–98, New York, NY, USA, 2019. Association for Computing Machinery.
 - [10] M. Yang, M. T. Isufi, E. and Schaub, and G. Leus. *IEEE Transactions on Signal Processing*, 2021-August:4633–4648, 2022.
 - [11] R. K. J. Wei, J. Wee, V. E. Laurent, and K. Xia. *Scientific Reports*, 12(1), 2022.
 - [12] F. Battiston, G. Cencetti, I. Iacopini, V. Latora, M. Lucas, A. Patania, J-G. Young, and G. Petri. *Physics Reports*, 874:1–92, 2020.
 - [13] F. Battiston, E. Amico, A. Barrat, G. Bianconi, G. F. de Arruda, B. Franceschiello, I. Iacopini, S. Kéfi, V. Latora, Y. Moreno, M. M. Murray, T. P. Peixoto, F. Vaccarino, and G. Petri. *Nature Physics*, 17(10):1093–1098, 2021.
 - [14] G. Bianconi. *Higher-Order Networks*. Elements in the Structure and Dynamics of Complex Networks. Cambridge University Press, 2021.
 - [15] S. Majhi, M. Perc, and D. Ghosh. *Journal of the Royal Society Interface*, 19(188), 2022.
 - [16] C. Bick, E. Gross, H. A. Harrington, and M. T. Schaub. *SIAM Review*, 65(3):686–731, 2023.
 - [17] T. Haruna and Y. Fujiki. *Frontiers in Neural Circuits*, 10(9), 2016.
 - [18] D. V. Anand and M. K. Chung. H. *IEEE Transactions on Medical Imaging*, 42(5):1563–1573, 2023.
 - [19] A. P. Millán, J. J. Torres, and G. Bianconi. *Physical Review Letters*, 124(21), 2020.

- [20] T. Carletti, L. Giambagli, and G. Bianconi. Phys. Rev. Lett., 130:187401, May 2023.
- [21] S. Barbarossa and S. Sardellitti. IEEE Transactions on Signal Processing, 68:2992–3007, 2020.
- [22] S. Ebli, M. Defferrard, and G. Spreemann. Simplicial neural networks, 2020. arXiv:2010.03633.
- [23] M. T. Schaub, Y. Zhu, J. B. Seby, T. M. Roddenberry, and S. Segarra. Signal Processing, 187, 2021.
- [24] R. B. Austin, F. G. David, and J. Leskovec. Science, 353(6295):163–166, 2016.
- [25] J. Grilli, G. Barabás, M.J. Michalska-Smith, and S. Allesina. Nature, 548(7666):210–213, Aug 2017.
- [26] E. Tekin, C. White, T. M. Kang, N. Singh, M. Cruz-Loya, R. Damoiseaux, V. M. Savage, and P. J. Yeh. npj Systems Biology and Applications, 4(1):31, Sep 2018.
- [27] N. Wiebe, D. Braun, and S. Lloyd. Phys. Rev. Lett., 109:050505, Aug 2012.
- [28] Y. Liu and S. Zhang. Theoretical Computer Science, 657:38–47, 2017. Frontiers of Algorithmics.
- [29] M. Ding, R. Kyng, M. P. Gutenberg, and P. Zhang. In Leibniz International Proceedings in Informatics, LIPIcs, volume 229. Schloss Dagstuhl- Leibniz-Zentrum für Informatik GmbH, Dagstuhl Publishing, 2022.
- [30] G. Schwarz. Hodge Decomposition - A Method for Solving Boundary Value Problems. Lecture Notes in Mathematics. Springer-Verlag Berlin, 1995.
- [31] D. N. Arnold, R. S. Falk, and R. Winther. Acta Numerica, 15:1–155, 2006.
- [32] D. A. Spielman and S.-H. Teng. In Proceedings of the Thirty-Sixth Annual ACM Symposium on Theory of Computing, STOC '04, page 81–90, New York, NY, USA, 2004. Association for Computing Machinery.
- [33] D. A. Spielman and S.-H. Teng. SIAM Journal on Matrix Analysis and Applications, 35(3):835–885, 2014.
- [34] M. B Cohen, B. T. Fasy, G. L. Miller, A. Nayyeri, R. Peng, and N. Walkington. In SODA '14: Proceedings of the twenty-fifth annual ACM-SIAM symposium on Discrete algorithms, 2014.
- [35] M. Black and A. Nayyeri. In Leibniz International Proceedings in Informatics, LIPIcs, volume 229. Schloss Dagstuhl- Leibniz-Zentrum für Informatik GmbH, Dagstuhl Publishing, 2022.
- [36] S. Chakraborty, A. Gilyén, and S. Jeffery. In 46th International Colloquium on Automata, Languages, and Programming (ICALP 2019), volume 132 of Leibniz International Proceedings in Informatics (LIPIcs), pages 33:1–33:14, Dagstuhl, Germany, 2019. Schloss Dagstuhl – Leibniz-Zentrum für Informatik.
- [37] I. Kerenidis and A. Prakash. In Leibniz International Proceedings in Informatics, LIPIcs, volume 67. Schloss Dagstuhl- Leibniz-Zentrum für Informatik GmbH, Dagstuhl Publishing, 2017.
- [38] S. Chakraborty, A. Morolia, and A. Peduri. Quantum, 7:988, April 2023.
- [39] A. Ambainis. In Christoph Dürr and Thomas Wilke, editors, 29th International Symposium on Theoretical Aspects of Computer Science (STACS 2012), volume 14 of Leibniz International Proceedings in Informatics (LIPIcs), pages 636–647, Dagstuhl, Germany, 2012. Schloss Dagstuhl – Leibniz-Zentrum für Informatik.
- [40] I. Kerenidis and A. Prakash. Quantum machine learning with subspace states, 2022. arXiv:2202.00054.
- [41] D. W. Berry, Y. Su, C. Gyurik, R. King, J. Basso, A. D. T. Barba, A. Rajput, N. Wiebe, V. Dunjko, and R. Babbush. PRX Quantum, 5, Feb 2024.
- [42] C. M. G. Leditto, A. Southwell, B. Tonekaboni, G. A. L. White, M. Usman, and K. Modi, 2023. arxiv:2312.07672.
- [43] S. Lloyd, S. Garnerone, and P. Zanardi. Nat. Comm., 7, 2016.
- [44] A. Gilyén, Y. Su, G. H. Low, and N. Wiebe. In Proceedings of the Annual ACM Symposium on Theory of Computing, 2019.
- [45] J. M. Martyn, Z. M. Rossi, A. K. Tan, and I. L. Chuang. PRX Quantum, 2(4), 2021.
- [46] S. McArdle, A. Gilyén, and M. Berta, 2022. arXiv:2209.12887.
- [47] S. A. Metwalli, F. Le Gall, and R. Van Meter. IEEE Transactions on Quantum Engineering, 1:1–11, 2021.
- [48] I. Y. Akhalwaya, S. Ubaru, K. L. Clarkson, M. S. Squillante, V. Jejjala, Y-H. He, K. Naidoo, V. Kalantzis, and L. Horesh. In The Twelfth International Conference on Learning Representations, 2024.
- [49] R. Hayakawa. Quantum, 6, 2022.
- [50] M. Yang, E. Isufi, M. T. Schaub, and G. Leus. In European Signal Processing Conference, volume 2021-August, pages 2005–2009. European Signal Processing Conference, EUSIPCO, 2021.
- [51] A. W. Harrow, A. Hassidim, and S. Lloyd. Quantum algorithm for linear systems of equations. Physical Review Letters, 103(15), 2009.
- [52] L. Lin. 2022. arXiv:2201.08309.
- [53] J. van Apeldoorn, A. Cornelissen, A. Gilyén, and G. Nannicini. In Proceedings of the 2023 Annual ACM-SIAM Symposium on Discrete Algorithms (SODA), pages 1265–1318, 2023.
- [54] N-H. Chia, A. Gilyén, T. Li, H-H. Lin, E. Tang, and C. Wang. In Proceedings of the 52nd Annual ACM SIGACT Symposium on Theory of Computing, STOC 2020, page 387–400, New York, NY, USA, 2020. Association for Computing Machinery.
- [55] E. Tang. Phys. Rev. Lett., 127:060503, Aug 2021.
- [56] S. Gharibian and F. Le Gall. In Proceedings of the Annual ACM Symposium on Theory of Computing, pages 19–32. Association for Computing Machinery, 2022.
- [57] S. Apers, S. Gribling, S. Sen, and D. Szabó. Quantum, 7:1202, December 2023.
- [58] T. E Goldberg. Combinatorial laplacians of simplicial complexes. Senior Thesis, Bard College, 6, 2002.
- [59] S. Garnerone, P. Zanardi, and D. A. Lidar. Phys. Rev. Lett., 108:230506, Jun 2012.
- [60] E. Sánchez-Burillo, J. Duch, J. Gómez-Gardeñes, and D. Zueco. Sci. Rep., 2(1):605, Aug 2012.
- [61] J. A. Acebrón, L. L. Bonilla, C. J. Pérez Vicente, and R. Ritort, F. and Spigler. Rev. Mod. Phys., 77:137–185, Apr 2005.
- [62] C. J. Cotter and J. Thuburn. Journal of Computational Physics, 257:1506–1526, 2014. Physics-compatible numerical methods.
- [63] K. B. Nakshatrala A. N. Hirani and J. H. Chaudhry. Numerical method for darcy flow derived using discrete exterior calculus. International Journal for Computational Methods in Engineering Science and Mechanics, 16(3):151–169, 2015.
- [64] S. M. Mamdouh, A. N. Hirani, and R. Samtaney. Journal of Computational Physics, 312:175–191, 2016.
- [65] J. Squire, H. Qin, and W. M. Tang. Physics of Plasmas, 19(8):084501, Aug 2012.

- [66] M. Kraus, K. Kormann, P. J. Morrison, and E. Sonnendrücker. *Journal of Plasma Physics*, 83(4):905830401, 2017.
- [67] S. Abramsky and A. Brandenburger. *New Journal of Physics*, 13(11):113036, nov 2011.
- [68] S. Abramsky, R. S. Barbosa, and S. Mansfield. *Phys. Rev. Lett.*, 119:050504, Aug 2017.
- [69] J. Nokkala, J. Piilo, and G. Bianconi. *Journal of Physics A: Mathematical and Theoretical*, 2024.
- [70] I. Y. Akhalwaya, Y-H. He, L. Horesh, V. Jejjala, W. Kirby, K. Naidoo, and S. Ubaru. *Physical Review A*, 106(2), 2022.
- [71] D. Horak and J. Jost. Spectra of combinatorial Laplace operators on simplicial complexes. *Advances in Mathematics*, 244, 2013.
- [72] D. W. Berry, A. M. Childs, R. Cleve, R. Kothari, and R. D. Somma. In *Proceedings of the Forty-Sixth Annual ACM Symposium on Theory of Computing, STOC '14*, page 283–292, New York, NY, USA, 2014. Association for Computing Machinery.

I. REVIEW ON SIMPLICIAL COMPLEXES

Here we give a brief overview of the necessary topology required to understand topological signal processing and k -HodgeRank; for a more detailed review of simplicial complexes and related algebraic topology see [58]. A simplicial complex with node set $\mathcal{V} = \{v_1, \dots, v_n\}$, which we denote by \mathcal{K}_n (sometimes dropping the n subscript), is a set of subsets of the node/vertex set \mathcal{V} (these subsets are called simplices) such that (i) $\{v_i\} \in \mathcal{K}_n$ for all $i \in \{1, \dots, n\}$, and (ii) if $\sigma \in \mathcal{K}_n$ and $\tau \subset \sigma$, then $\tau \in \mathcal{K}_n$ (i.e., every subset of a simplex is a simplex). A particular family of simplicial complexes that are relevant to this work is the family of clique complexes. A clique complex $\mathcal{K}_n(\mathcal{G})$, for some graph \mathcal{G} , is a simplicial complex with the same node set as \mathcal{G} where the set of k -simplices is the set of $(k-1)$ -cliques in \mathcal{G} . The structure of $\mathcal{K}_n(\mathcal{G})$ is thus entirely determined by the graph \mathcal{G} .

We give some basic terminology here that we use when discussing simplicial complexes. A simplex $\sigma \in \mathcal{K}_n$ is called a k -simplex if $|\sigma| = k+1$ (the $+1$ follows from the idea that a k -dimensional simplex in the geometric sense has $k+1$ vertices, e.g. a 2-dimensional simplex is a triangle which has 3 vertices). A simplex τ is a q -face of a k -simplex σ if $\tau \subset \sigma$ and $|\tau| = q+1$, for $q < k$. To construct the boundary operators, we also associate an orientation to each simplex, which corresponds to the parity of a permutation of its constituent elements. That is, each simplex has two orientations, which are called positive or negative. For a simplex $\sigma = \{v_{i_0}, \dots, v_{i_k}\}$, we denote the oriented simplex by $[v_{i_0}, \dots, v_{i_k}]$.

Simplicial complexes are a well-studied class of higher-order networks because of their extra topological structure. One particularly relevant construction from algebraic topology associated to simplicial complexes that mathematically underpins our work is the space of k -chains $\mathfrak{C}_k := \mathfrak{C}_k(\mathcal{K})$ of a simplicial complex \mathcal{K} , defined as formal sums of k -simplices in the complex. It is sufficient for our purposes to consider the space of k -chains as (isomorphic to) a real vector space \mathbb{R}^{n_k} where the basis is the set of k -simplices in \mathcal{K} , i.e., $\mathfrak{C}_k := \{\sum_{i=0}^{n_k-1} c_i \sigma_k^i \mid c_i \in \mathbb{R}\}$, where n_k is the number of k -simplices in \mathcal{K} . The isomorphism to \mathbb{R}^{n_k} can be seen by mapping each simplex σ_k^i to \mathbf{e}_i , where $\{\mathbf{e}_i\}_{i \in [n_k]}$ is the standard basis for \mathbb{R}^{n_k} .

The different spaces $\mathfrak{C}_k(\mathcal{K})$ associated with different dimensions k are related to each other by maps known as boundary operators. The k -th boundary operator $\partial_k : \mathfrak{C}_k \rightarrow \mathfrak{C}_{k-1}$ is a linear map such that for $\sigma_k = [v_{i_0}, \dots, v_{i_k}] \in \mathfrak{C}_k$,

$$\partial_k \sigma_k := \sum_{j=0}^k (-1)^j [v_{i_0}, \dots, v_{i_{j-1}}, v_{i_{j+1}}, \dots, v_{i_k}]. \quad (11)$$

Here, the vertex v_{i_j} is removed from each simplex in the sum. That is, ∂_k maps a k -simplex to a formal sum of its $(k-1)$ -faces, which are the boundary of the k -simplex in a topological sense.

Since the boundary operator acts linearly on the space of k -chains, it can be represented by a matrix. Let $\mathbf{B}_k : \mathbb{R}^{n_k} \rightarrow \mathbb{R}^{n_{k-1}}$ be the matrix representation of ∂_k , using the canonical bases of k -simplices and $(k-1)$ -simplices for $\mathfrak{C}_k(\mathcal{K})$ and $\mathfrak{C}_{k-1}(\mathcal{K})$ respectively. The entries of \mathbf{B}_k are

$$(\mathbf{B}_k)_{ij} = \begin{cases} 1, & \text{if } i \neq j, \sigma_{k-1}^i \subset \sigma_k^j, \epsilon(\sigma_{k-1}^i) \sim \epsilon(\sigma_k^j) \\ -1, & \text{if } i \neq j, \sigma_{k-1}^i \subset \sigma_k^j, \epsilon(\sigma_{k-1}^i) \approx \epsilon(\sigma_k^j) \\ 0, & \text{otherwise,} \end{cases} \quad (12)$$

where $\epsilon(\sigma_{k-1}^i) \sim \epsilon(\sigma_k^j)$ means σ_{k-1}^i and σ_k^j have the same orientation and $\epsilon(\sigma_{k-1}^i) \approx \epsilon(\sigma_k^j)$ means σ_{k-1}^i and σ_k^j have different orientations (again referring to [58] for the full definition). The ± 1 entries account for the orientation of each k -simplex relative to its boundary $(k-1)$ -faces. The adjoint (equivalently transpose since \mathbf{B}_k is real) of the boundary operator \mathbf{B}_k^\dagger is called the coboundary operator and naturally maps from $\mathbb{R}^{n_{k-1}}$ ($\mathfrak{C}_{k-1}(\mathcal{K})$) to \mathbb{R}^{n_k} ($\mathfrak{C}_k(\mathcal{K})$).

The boundary and coboundary operators are used to construct the Hodge Laplacian (matrix) \mathbf{L}_k , defined as

$$\mathbf{L}_k := \begin{cases} \mathbf{B}_{k+1}\mathbf{B}_{k+1}^\dagger, & \text{for } k = 0 \\ \mathbf{B}_k^\dagger\mathbf{B}_k + \mathbf{B}_{k+1}\mathbf{B}_{k+1}^\dagger, & \text{for } 1 < k < n - 2 \\ \mathbf{B}_k^\dagger\mathbf{B}_k, & \text{for } k = n - 1. \end{cases} \quad (13)$$

Furthermore, $\mathbf{L}_k^\ell := \mathbf{B}_k^\dagger\mathbf{B}_k$ and $\mathbf{L}_k^u := \mathbf{B}_{k+1}\mathbf{B}_{k+1}^\dagger$ are defined as lower and upper Hodge Laplacian operators, respectively. More details of these operators can be found in Ref. [58]. Hence, Eq. (2) can be expressed as $\mathbf{s}_*^{k-1} = (\mathbf{L}_{k-1}^u)^\dagger \mathbf{B}_k \mathbf{s}^k$.

The boundary and Laplacian operators define what is known as the Hodge decomposition. This states that \mathbb{R}^{n_k} , the vector space of real numbers assigned to k -simplices (i.e. the space of k -chains), can be partitioned into three orthogonal components

$$\mathbb{R}^{n_k} = \text{im}(\mathbf{B}_k^\dagger) \oplus \text{im}(\mathbf{B}_{k+1}) \oplus \ker(\mathbf{L}_k). \quad (14)$$

These are respectively known as the gradient, curl, and harmonic components, generalizing the language used in low-dimensional vector calculus. For an arbitrary $\mathbf{s}^k \in \mathbb{R}^{n_k}$, we write $\mathbf{s}^k = \mathbf{s}_G^k + \mathbf{s}_C^k + \mathbf{s}_H^k$ where \mathbf{s}_G^k , \mathbf{s}_C^k , and \mathbf{s}_H^k belong to the respective subspaces. The dimension of $\ker(\mathbf{L}_k)$ is known as the k -th Betti number of the simplicial complex \mathcal{K}_n , and is well studied in classical and quantum topological data analysis.

II. TOPOLOGICAL SIGNAL PROCESSING (TSP) AND DETAILS OF QUANTUM TOPOLOGICAL SIGNAL PROCESSING (QTSP)

We utilize a newly developed framework from signal processing called topological signal processing (TSP) [21] to design our algorithms. TSP extends the concept of signals and signal processing from discretized time domains to more topologically nuanced spaces. In the TSP framework, the signal is referred to as a simplicial signal $\mathbf{s}^k \in \mathbb{R}^{n_k}$ and is defined as a k -chain (formally, a k -cochain, but for our purposes these are isomorphic) on a simplicial complex \mathcal{K}_n , effectively assigning a real number to each k -simplex. To perform filtering operations on these signals that respect the topology of the underlying space, TSP employs a filter operator described by polynomials of lower and upper Hodge Laplacian operators $\mathbf{L}_k^\ell = \mathbf{B}_k^\dagger\mathbf{B}_k$ and $\mathbf{L}_k^u = \mathbf{B}_{k+1}\mathbf{B}_{k+1}^\dagger$ [10, 50], respectively, called a simplicial filter:

$$H(\mathbf{L}_k^\ell, \mathbf{L}_k^u) := \sum_{i_\ell=1}^{d_\ell} h_{i_\ell}^\ell (\mathbf{L}_k^\ell)^{i_\ell} + \sum_{i_u=1}^{d_u} h_{i_u}^u (\mathbf{L}_k^u)^{i_u} - h_0 \mathbf{I}.$$

The aim of TSP is to design such a filter $H(x, y)$ so that the filtered simplicial signal $\mathbf{s}_{\text{fil}}^k := H(\mathbf{L}_k^\ell, \mathbf{L}_k^u) \mathbf{s}^k$ extracts particular information from the original signal \mathbf{s}^k . The form of the filter is determined by its polynomial coefficients, called the simplicial filter coefficients, and depends on the task at hand. The problem of finding the coefficients is known as the filter design problem. Yang et al. [10] designed simplicial filters to project a simplicial signal \mathbf{s}^k onto signals $\mathbf{B}_k^\top \mathbf{s}^{k-1}$ and $\mathbf{B}_{k+1} \mathbf{s}^{k+1}$, which are similar to gradient and curl projections that we discuss in Application 1. However, the polynomials they use to approximate the projections are quite different to what we employ in this paper, as they used least squares methods to find the filter coefficients. Nevertheless, this particular application helps illustrate the connections between the Hodge decomposition and k -HodgeRank.

Recently a quantum algorithm, called quantum topological signal processing (QTSP), was developed for performing TSP filtering on quantum computers. Here we briefly review the general QTSP filtering algorithm, and refer the interested reader to [42] for more details. For our purposes in this paper, we slightly generalize the definition of a simplicial filter given in their paper to accommodate the “filter” we implement in quantum k -HodgeRank. As in Lemma 1 of [42], define $H(x, y) : [-1, 1]^2 \rightarrow [-1, 1]$ as a multivariable polynomial that is the sum of $p(x)$ and $q(y)$, each with degree at most D such that both polynomials are either both even, both odd, or one is zero. The definite parity of H ensures that $H(\mathbf{B}_k, \mathbf{B}_{k+1}^\dagger)$ is a map from \mathbb{R}^{n_k} to \mathbb{R}^{n_j} for some $j \in \{k-1, k, k+1\}$ (that is, the output simplicial signals all correspond to simplices of the same dimension).

Instead of encoding each entry of the boundary matrices via QRAM/SAIM to implement block-encoding of \mathbf{B}_k and \mathbf{B}_{k+1}^\dagger , a projected unitary encoding of \mathbf{B}_k and \mathbf{B}_{k+1}^\dagger is used. This is done using what is known as the fermionic Dirac boundary operator representation [70], which we denote \mathbf{D} . Using its efficient application via a Clifford loader circuit

as described in [40], the PUE of \mathbf{B}_k is given by

$$\Pi_{k-1} \mathbf{D} \Pi_k = \frac{\mathbf{B}_k}{\sqrt{n}}, \quad (15)$$

where Π_k is a k -simplex identifying function, given in [41, 46, 47], such that

$$\Pi_k |\sigma_k^i\rangle |0\rangle = \begin{cases} |\sigma_k^i\rangle |1\rangle, & \text{if } \sigma_k^i \in \mathcal{K}_n \\ |\sigma_k^i\rangle |0\rangle, & \text{if } \sigma_k^i \notin \mathcal{K}_n. \end{cases}$$

The quantum circuit for D does not depend on the dimension of the simplices, or even the simplicial complex itself. On the other hand, Π_k is a sequence of multi-controlled CNOT gates determined by the adjacency matrix of the underlying graph \mathcal{G} , along with inequality checks against predetermined values that depend on k . This is done via classical control, as we assume the adjacency matrix is given classically, without using QRAM/SAIM. We refer to this computational model as a classically controlled quantum circuit, as defined in the main body. Then, the quantum singular value transformation (QSVT) and linear combination of unitaries (LCU) methods provide a way of constructing a PUE of the simplicial filter operator $H\left(\mathbf{B}_k/\sqrt{n}, \mathbf{B}_{k+1}^\dagger/\sqrt{n}\right)$ given by

$$p\left(\frac{\mathbf{B}_k}{\sqrt{n}}\right) + q\left(\frac{\mathbf{B}_{k+1}^\dagger}{\sqrt{n}}\right) := \sum_{i_\ell \in [d_\ell]} \mathfrak{h}_{i_\ell}^\ell \left(\frac{\mathbf{B}_k}{\sqrt{n}}\right)^{i_\ell} + \sum_{i_u \in [d_u]} \mathfrak{h}_{i_u}^u \left(\frac{\mathbf{B}_{k+1}^\dagger}{\sqrt{n}}\right)^{i_u}. \quad (16)$$

This generalizes the definition in [42], which is standard in classical TSP literature, as we do not restrict the filter to be a summation of polynomials of \mathbf{L}_k^ℓ and \mathbf{L}_k^u (which is equivalent to assuming that both i_ℓ and i_u are even). In [42], it is shown that one can construct the quantum circuit QTSP($k, \mathcal{K}_n, H(x, y)$) using $a = n + 6$ ancilla qubits such that

$$\text{QTSP}(k, \mathcal{K}_n, H(x, y))(|s^k\rangle |0\rangle^{\otimes a}) = |0\rangle^{\otimes a} H\left(\frac{\mathbf{B}_k}{\sqrt{n}}, \frac{\mathbf{B}_{k+1}^\dagger}{\sqrt{n}}\right) |s^k\rangle + |\perp\rangle, \quad (17)$$

where $|\perp\rangle$ is an un-normalized state satisfying $(\mathbf{1}^n \otimes \langle 0|^{\otimes a}) |\perp\rangle = 0$, and $|s^k\rangle$ is as defined in Eq. (3). One can consider QTSP($k, \mathcal{K}_n, H(x, y)$) as an implementation of QSVT [44] with a function $H(x, y)$ and PUEs of \mathbf{B}_k and \mathbf{B}_{k+1}^\dagger [40, 46]. Upon successful postselection, the output state is given in Eq. (4). This algorithm, excluding post selection, has non-Clifford gate depth $O(Dn \log(n))$ and uses n system qubits (as described in Eq. (18)) and $O(n)$ ancilla qubits [42].

To complete the definition of s^k given in Eq. (3), here we give the definition of $|\sigma_k^i\rangle$, as originally defined in [43]. Recall that σ_k^i is a $(k+1)$ -element subset of $[n]$. Suppose that $\sigma_k^i = \{v_{i_0}, \dots, v_{i_k}\}$. Then

$$|\sigma_k^i\rangle = \bigotimes_{j=1}^n |u_j\rangle, \quad u_j = \begin{cases} 1 & v_{i_j} \in \sigma_k^i \\ 0 & \text{otherwise.} \end{cases} \quad (18)$$

In other words, $|\sigma_k^i\rangle$ is an n -qubit computational basis state where the j -th qubit is 1 if and only if vertex v_j is in the set σ_k^i .

III. QUANTUM HODGERANK (EXTENDED)

Problem 1. *Given a simplicial signal state $|s^k\rangle$ that encodes a simplicial signal value s_i^k for each k -simplex σ_k^i , output a quantum state that has amplitudes proportional to Eq. (2).*

The quantum k -HodgeRank algorithm is essentially an implementation of the QTSP algorithm. Quantum k -HodgeRank outputs, upon successful post-selection, a quantum state that encodes an approximation to the (normalised) vector in Eq. (2).

Let $\mathbf{U}_\mathbf{A}$ be a block-encoding or a projected unitary encoding of a matrix \mathbf{A} . Gilyen et al. [44] apply QSVT to create a quantum circuit that encodes \mathbf{A}^\dagger , the Moore-Penrose pseudoinverse of \mathbf{A} . For simplicity, we use the slight modification of the statement as given in [49] (in the proof of their Theorem 5), which assumes \mathbf{A} is Hermitian. The idea is to implement QSVT with a polynomial $g_\varepsilon(x)$ of degree $O(\kappa_k \log(\kappa/(\alpha\varepsilon)))$, where $\kappa \in (\sqrt{n}/\zeta_{\min}, \infty)$ and

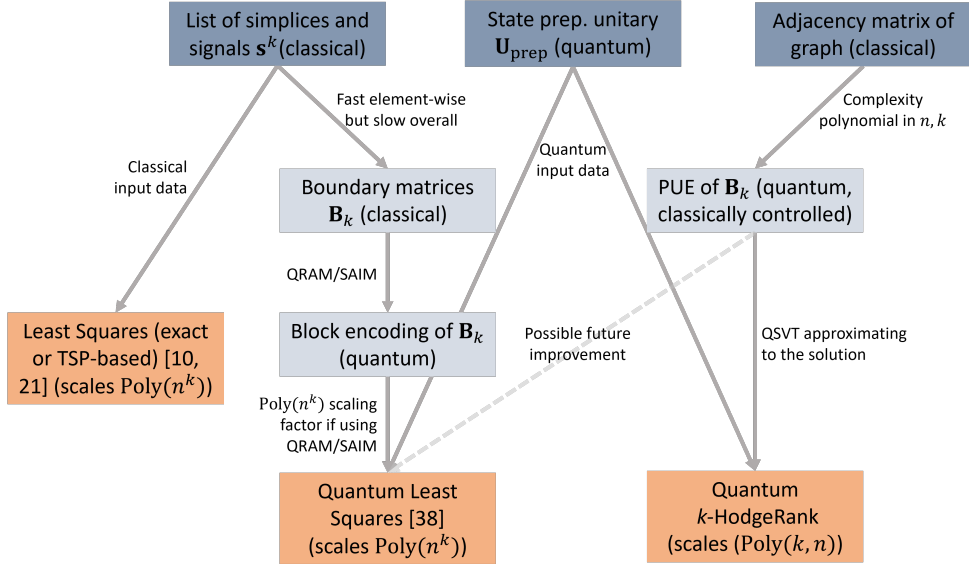


Figure 1. A comparison between several quantum least square (QLS) algorithms (with or without block-encoding (BE) method) and quantum k -HodgeRank to solve the k -HodgeRank problem given an input simplicial signal state $|\mathbf{s}^k\rangle$. Compared to classical methods, we do not need to explicitly construct the boundary operator element-wise, nor do we need to perform classical matrix-matrix or matrix-vector multiplication. Compared to general quantum least squares algorithms, such as those given by [38], quantum HodgeRank utilizes a method that constructs an operator that encodes the boundary matrix with a much smaller scaling factor, which leads to much faster computations if the clique complex has many k -simplices. While it is possible that the methods used in [38] could be extended to utilize the PUE of \mathbf{B}_k , we do not explore that in this work.

$\varepsilon \in (0, 1/2)$, such that (i) $|g_\varepsilon(x)| \leq 1$ for all $x \in [-1, 1]$, (ii) $|1/x - 2\kappa g_\varepsilon(x)| \leq \varepsilon$ for $x \in [-1, -1/\kappa] \cup [1/\kappa, 1]$, and (iii) $g_\varepsilon(0) = 0$. Applying $g_\varepsilon(x)$ to \mathbf{A} approximately inverts every non-zero singular value while leaving the zero values untouched. Thus, it follows that $\|\mathbf{A}^+ - 2\kappa/\alpha(\mathbf{1}^a \otimes \langle 0 |^{\otimes n}) \mathbf{U}_A (\mathbf{1}^a \otimes |0\rangle^{\otimes n})\|_2 \leq \varepsilon$.

In the k -HodgeRank problem, we want to implement $(\mathbf{B}_k \mathbf{B}_k^\dagger)^+ \mathbf{B}_k$, given a PUE of \mathbf{B}_k . This is naturally related to implementing the Moore-Penrose pseudoinverse of $\mathbf{B}_k \mathbf{B}_k^\dagger$, which is a Hermitian matrix. It immediately follows that each eigenvalue of $\mathbf{B}_k \mathbf{B}_k^\dagger$ is the square of the corresponding singular value of \mathbf{B}_k . Thus, we use QSVT to implement the polynomial $xg_\varepsilon(x^2)$. Note that (i) since $|g_\varepsilon(x)| \leq 1$ for all $x \in [-1, 1]$, it immediately follows that $|xg_\varepsilon(x^2)| \leq 1$ for all $x \in [-1, 1]$, and (ii) if $g_\varepsilon(x)$ has degree D , then $xg_\varepsilon(x^2)$ has degree $2D + 1$. This allows the tools developed in the proof of Theorem 5 in [49] to be applied even though \mathbf{B}_k is not Hermitian (and indeed not even necessarily square). This is discussed briefly in [42]. Recall that the action of the QTSP circuit is described in Eq. (17). The circuit to apply QTSP($k, \mathcal{K}_n, xg_\varepsilon(x^2)$) then has non-Clifford gate depth $O(n\kappa_k^2 \log(n) \log(\sqrt{n}\kappa_k^2/\varepsilon))$, as stated in Eq. (8), which follows from the cost of QTSP given in Appendix II with $D = O(\kappa_k^2 \log(\sqrt{n}\kappa_k^2/\varepsilon))$. Recall that κ_k is the effective condition number of \mathbf{B}_k and let ζ_{\min}^k be the smallest non-zero singular value of \mathbf{B}_k . Problem 1 can be approximately solved as described in the following theorem.

Theorem 1. Fix $\varepsilon \in (0, \mathcal{N}_*)$. Upon correct postselection, the QTSP algorithm with input state $|\mathbf{s}^k\rangle$ and $H(x, y) = p(x) = xg_\varepsilon(x^2)$ outputs a quantum state $|\tilde{\mathbf{s}}_*^{k-1}\rangle$ that is $2\varepsilon/(\mathcal{N}_* - \varepsilon)$ -close to $|\mathbf{s}_*^{k-1}\rangle := 1/\mathcal{N}_* (\mathbf{B}_k \mathbf{B}_k^\dagger)^+ \mathbf{B}_k |\mathbf{s}^k\rangle$. The cost of applying QTSP($k, \mathcal{K}_n, xg_\varepsilon(x^2)$) is $O(\kappa_k^2 n \log(n) \log(\sqrt{n}\kappa_k^2/\varepsilon))$ and the probability of successful postselection is $O(n\mathcal{N}_*^2/\kappa_k^4)$, where $\mathcal{N}_* := \|(\mathbf{B}_k \mathbf{B}_k^\dagger)^+ \mathbf{B}_k |\mathbf{s}^k\rangle\|_2$.

Proof. It follows from [42] (adapting Theorem 5 in [49]) that there exists a polynomial $p(x) = xg_\varepsilon(x^2)$ of degree $O(\kappa_k^2 \log(\sqrt{n}\kappa_k^2/\varepsilon))$ satisfying $\kappa_k \in (\sqrt{n}/\zeta_{\min}^k, \infty)$ and $\varepsilon \in (0, 1/2)$, such that $|g_\varepsilon(x)| \leq 1$ and $|xg_\varepsilon(x^2)|$ for all $x \in [-1, 1]$ and $|1/x - 2\kappa_k^2 g_\varepsilon(x)| \leq \varepsilon$ for $x \in [-1, -1/\kappa_k^2] \cup [1/\kappa_k^2, 1]$. It follows that

$$\left\| (\mathbf{L}_{k-1}^u)^+ \mathbf{B}_k - \frac{2\kappa_k^2}{\sqrt{n}} p(\mathbf{B}_k/\sqrt{n}) \right\|_2 \leq \varepsilon, \quad (19)$$

recalling $\mathbf{L}_{k-1}^u = \mathbf{B}_k \mathbf{B}_k^\dagger$ as defined in Appendix I. Also note that $|\mathbf{s}_*^{k-1}\rangle = \frac{(\mathbf{L}_{k-1}^u)^+ \mathbf{B}_k |\mathbf{s}^k\rangle}{\|(\mathbf{L}_{k-1}^u)^+ \mathbf{B}_k |\mathbf{s}^k\rangle\|}$ is an alternative expression for $|\mathbf{s}_*^{k-1}\rangle$ as defined in Eq. (5). Thus, we can apply QTSP($k, \mathcal{K}_n, xg_\varepsilon(x^2)$) to the input state and the ancilla qubits

such that

$$\text{QTSP}(k, \mathcal{K}_n, xg_\varepsilon(x^2))(|\mathbf{s}^k\rangle|0\rangle^{\otimes a}) = p(\mathbf{B}_k/\sqrt{n})|\mathbf{s}^k\rangle|0\rangle^{\otimes a} + |\perp\rangle. \quad (20)$$

Upon the successful postselection on the ancilla qubits with probability $O(\tilde{\mathcal{N}}_*^2)$, where $\tilde{\mathcal{N}}_* := \|p(\mathbf{B}_k/\sqrt{n})|\mathbf{s}^k\rangle\|_2$, the output is

$$|\tilde{\mathbf{s}}_*^{k-1}\rangle = \frac{1}{\tilde{\mathcal{N}}_*} p\left(\frac{\mathbf{B}_k}{\sqrt{n}}\right)|\mathbf{s}^k\rangle = \frac{1}{\tilde{\mathcal{N}}_*} \sum_{i \in [n_{k-1}]} \frac{\tilde{s}_{*,i}^{k-1}}{2\kappa_k^2/\sqrt{n}} |\sigma_{k-1}^i\rangle. \quad (21)$$

Eq. (20) and the assumption that $\mathcal{N}_* > \varepsilon$ together imply that $\tilde{\mathcal{N}}_* \geq \sqrt{n}(\mathcal{N}_* - \varepsilon)/(2\kappa_k^2)$, as the reverse triangle inequality implies that

$$\left\| p\left(\frac{\mathbf{B}_k}{\sqrt{n}}\right)|\mathbf{s}^k\rangle \right\| = \left\| p\left(\frac{\mathbf{B}_k}{\sqrt{n}}\right)|\mathbf{s}^k\rangle - \frac{\sqrt{n}}{2\kappa_k^2} (\mathbf{L}_{k-1}^u)^\dagger \mathbf{B}_k |\mathbf{s}^k\rangle + \frac{\sqrt{n}}{2\kappa_k^2} (\mathbf{L}_{k-1}^u)^\dagger \mathbf{B}_k |\mathbf{s}^k\rangle \right\| \geq \frac{\sqrt{n}}{2\kappa_k^2} |\mathcal{N}_* - x|$$

for some $x \in (0, \varepsilon)$, which implies the desired lower bound on $\tilde{\mathcal{N}}_*$. A similar argument implies the corresponding upper bound of $\tilde{\mathcal{N}}_* \leq \sqrt{n}(\mathcal{N}_* + \varepsilon)/(2\kappa_k^2)$. It follows that

$$\begin{aligned} \left\| |\mathbf{s}_*^{k-1}\rangle - |\tilde{\mathbf{s}}_*^{k-1}\rangle \right\|_2 &= \left\| \frac{(\mathbf{L}_{k-1}^u)^\dagger \mathbf{B}_k |\mathbf{s}^k\rangle}{\mathcal{N}_*} - \frac{p(\mathbf{B}_k/\sqrt{n})|\mathbf{s}^k\rangle}{\tilde{\mathcal{N}}_*} \right\|_2 \\ &= \frac{1}{\mathcal{N}_* \tilde{\mathcal{N}}_*} \left\| \frac{\sqrt{n}}{2\kappa_k^2} \tilde{\mathcal{N}}_* (\mathbf{L}_{k-1}^u)^\dagger \mathbf{B}_k |\mathbf{s}^k\rangle - \mathcal{N}_* p(\mathbf{B}_k/\sqrt{n})|\mathbf{s}^k\rangle \right\| \\ &\leq \frac{1}{\tilde{\mathcal{N}}_*} \left[\left\| \frac{\sqrt{n}}{2\kappa_k^2} (\mathbf{L}_{k-1}^u)^\dagger \mathbf{B}_k |\mathbf{s}^k\rangle - p(\mathbf{B}_k/\sqrt{n})|\mathbf{s}^k\rangle \right\| + \frac{\sqrt{n}}{2\kappa_k^2} \varepsilon \right] \\ &\leq \frac{1}{\mathcal{N}_* - \varepsilon} \left[\left\| (\mathbf{L}_{k-1}^u)^\dagger \mathbf{B}_k |\mathbf{s}^k\rangle - \frac{2\kappa_k^2}{\sqrt{n}} p(\mathbf{B}_k/\sqrt{n})|\mathbf{s}^k\rangle \right\| + \varepsilon \right] \\ &\leq \frac{2\varepsilon}{\mathcal{N}_* - \varepsilon}. \end{aligned}$$

This proves the first claim of the theorem. Now we turn to the postselection probability. The probability of successful postselection (that is, obtaining $|\tilde{\mathbf{s}}_*^{k-1}\rangle$), is $\tilde{\mathcal{N}}_*^2$. By the aforementioned bounds on $\tilde{\mathcal{N}}_*$, if $\tilde{\mathcal{N}}_* > \varepsilon$, this is $\Omega(n(\mathcal{N}_* - \varepsilon)^2/(2\kappa_k^2)^2)$. \square

We remark that \mathcal{N}_* can be arbitrarily small in general. However, if the consistency measure $R(k)$ is bounded away from zero, one can choose ε that is small enough so that $\| |\mathbf{s}_*^{k-1}\rangle - |\tilde{\mathbf{s}}_*^{k-1}\rangle \|_2$ does not blow up. Let γ_G be a (potentially application-dependent) lower bound for $R(k)$ set such that the rankability of $|\mathbf{s}_*^{k-1}\rangle$ is considered good (e.g. $\gamma_G = 0.1$). Then, for data \mathbf{s}^k such that $R(k) \geq \gamma_G$, it follows that

$$\gamma_G \leq \left\| \mathbf{B}_k^\dagger (\mathbf{L}_{k-1}^u)^\dagger \mathbf{B}_k |\mathbf{s}^k\rangle \right\|_2 \leq \left\| \mathbf{B}_k^\dagger \right\|_2 \mathcal{N}_* \leq \sqrt{n} \mathcal{N}_*,$$

since the largest singular value of \mathbf{B}_k is at most \sqrt{n} [71]. By setting $\varepsilon = \frac{1}{2}\gamma_* := \gamma_G/(2\sqrt{n})$, Theorem 1 ensures that quantum k -HodgeRank outputs a solution that is still $(4\varepsilon/\mathcal{N}_*)$ -close to $|\mathbf{s}_*^{k-1}\rangle$ in vector 2-norm upon correct postselection. In general, setting $\varepsilon = \frac{\varepsilon'}{4}\gamma_*$, for a sufficiently small choice of ε' , ensures that the output after postselection is ε' -close to $|\mathbf{s}_*^{k-1}\rangle$ in vector 2-norm since $\mathcal{N}_* - \varepsilon \geq \frac{\gamma_G}{\sqrt{n}}(1 - \varepsilon'/4)$. Since the complexity of $\text{QTSP}(k, \mathcal{K}_n, xg_\varepsilon(x^2))$ depends only logarithmically on ε , changing it by a factor of $\Omega(n^{-1/2})$ (if $\gamma_G = \Omega(1)$, for example) causes only a constant change in the complexity.

Moreover, if we want to boost the probability of successful postselection to be $O(1)$, we can implement $O(\kappa_k^2/(\sqrt{n}\gamma_*))$ rounds of (fixed-point oblivious) amplitude amplification [72]. Hence, the total non-Clifford gate depth of outputting $|\tilde{\mathbf{s}}_*^{k-1}\rangle$ that is $O(\varepsilon/\mathcal{N}_*)$ -close to $|\mathbf{s}_*^{k-1}\rangle$ with probability above $2/3$ is $O(\kappa_k^2 D \sqrt{n} \log(n)/\gamma_*)$.

A. Assumptions on the weights w_{ij} in the ℓ_2 minimization

Here we also discuss the assumption we make about w_{ij} in Eq. (1). Our quantum k -HodgeRank algorithm assumes that $w_{ij} = 1$ if $[v_i, v_j] \in \mathcal{E}$ and is 0 otherwise. This is equivalent to the condition that there exists some constant $c \in \mathbb{N}$

such that every pair of alternatives is either ranked by zero people or c people. This condition is called a *balanced* case in statistical ranking [4]. The primary reason for this restriction is because the boundary and coboundary operators in terms of fermionic Dirac operators, as originally given by [43, 48], are adjoint with respect to the standard unweighted inner product. Generalizing this without using QRAM/SAIM would require modification of the Dirac operator \mathbf{D} and would be an interesting avenue for further exploration.

IV. APPLICATION 1: CALCULATION OF HODGERANK (IN)CONSISTENCY MEASURES VIA ACCELERATED HADAMARD TESTS

Here we give more details on the approximation of the (generalized) consistency measure $R(k)$ and local inconsistency measure $R_C(k)$, as defined in Eq. (9). Since the methods for computing these are nearly identical, we combine their discussion. Let Π_P be a projector onto a particular subspace of \mathbb{R}^{n_k} , viewed as the space of k -chains. Here P is a placeholder for either G (projecting onto $\text{im}(\mathbf{B}_k^\dagger)$) or C (projecting onto $\text{im}(\mathbf{B}_{k+1})$). The orthogonality of the gradient, curl, and harmonic spaces given by the Hodge decomposition (Eq. 14) implies that

$$\langle \mathbf{s}^k | \Pi_P | \mathbf{s}^k \rangle = \frac{1}{\|\mathbf{s}^k\|^2} \langle \mathbf{s}^k, \mathbf{s}_P^k \rangle = \frac{\|\mathbf{s}_P^k\|^2}{\|\mathbf{s}^k\|^2}.$$

Thus, if we can obtain an ε -approximation to the inner product $\langle \mathbf{s}^k | \Pi_P | \mathbf{s}^k \rangle$, this is a $\sqrt{\varepsilon}$ -approximation to the relative length of the projection of \mathbf{s}^k onto the desired subspace. When $P = G$, this is the consistency measure, and when $P = C$ this is the local inconsistency measure.

Let $\mathbf{U}_{\Pi_P} := \text{QTSP}\left(k, \mathcal{K}_n, \frac{1}{2\kappa_P^2} \tilde{\Pi}_P\right)$ be the projected unitary encoding of the ε' -approximation to the projector $\frac{1}{2\kappa_P^2} \Pi_P$ (defined in Application 1 in the main text), where $\kappa_G = \kappa_k$ and $\kappa_C = \kappa_{k+1}$ are defined accordingly. Then

$$\text{QTSP}\left(k, \mathcal{K}_n, \frac{1}{2\kappa_P^2} \tilde{\Pi}_P\right) |0\rangle^{\otimes a} = \frac{1}{2\kappa_P^2} \tilde{\Pi}_P | \mathbf{s}^k \rangle |0\rangle^{\otimes a} + \sum_{x \neq 0} |\text{Garb}_x\rangle |x\rangle,$$

where $\|\Pi_P - \tilde{\Pi}_P\| \leq \varepsilon'$. This implies that

$$\langle \mathbf{s}^k | \langle 0 |^{\otimes a} \text{QTSP}\left(k, \mathcal{K}_n, \frac{1}{2\kappa_P^2} \tilde{\Pi}_P\right) | \mathbf{s}^k \rangle |0\rangle^{\otimes a} = \frac{1}{2\kappa_P^2} \langle \mathbf{s}^k | \tilde{\Pi}_P | \mathbf{s}^k \rangle.$$

Recall that if $\|\Pi - \tilde{\Pi}\| \leq \varepsilon'$, then $\left| \langle \Pi | x \rangle, |y\rangle \rangle - \langle \tilde{\Pi} | x \rangle, |y\rangle \rangle \right| \leq \varepsilon'$ for all unit vectors $|x\rangle, |y\rangle$. Applying this with $|x\rangle = |y\rangle = |\mathbf{s}^k\rangle$ implies that $\langle \mathbf{s}^k | \tilde{\Pi}_P | \mathbf{s}^k \rangle$ is an ε' -approximation to $\langle \mathbf{s}^k | \Pi_P | \mathbf{s}^k \rangle$.

Importantly, $\langle \mathbf{s}^k | \tilde{\Pi}_P | \mathbf{s}^k \rangle$ can be approximated via a Hadamard test to β additive error with probability at least $1 - \delta$ in $O(\log(1/\delta)/\beta^2)$ controlled applications of $\text{QTSP}\left(k, \mathcal{K}_n, \frac{1}{2\kappa_P^2} \tilde{\Pi}_P\right)$ and \mathbf{U}_{prep} . This can be improved to $O(\log(1/\delta)/\beta)$ applications using amplitude estimation, specifically by performing amplitude estimation on the Grover iterate that identifies the ancilla in state $|0\rangle^{\otimes a}$. The Grover iterate itself is straightforward to implement given the state preparation unitary \mathbf{U}_{prep} . Knowing $\frac{1}{2\kappa_P^2} \frac{\|\mathbf{s}_P^k\|^2}{\|\mathbf{s}^k\|^2}$ to additive error β corresponds to knowing $\frac{\|\mathbf{s}_P^k\|}{\|\mathbf{s}^k\|}$ to additive error $\kappa_P \sqrt{2\beta}$. Thus, using $O(\kappa_P^2 \log(1/\delta)/\varepsilon^2)$ applications of the QTSP implementation of the Hodge projector with approximation error $\varepsilon' = \frac{\varepsilon^2}{2}$, we can approximate $\frac{\|\mathbf{s}_P^k\|^2}{\|\mathbf{s}^k\|^2}$ to error ε with probability at least $1 - \delta$. Combining this with the complexity for implementing $\text{QTSP}(k, \mathcal{K}_n, H(x, y))$ as given in Eq. (8) (or Theorem 2 in [42]) gives the complexities stated in Application 2.

V. APPLICATION 2: FINDING THE RELATIVE RANKING OF ALTERNATIVES

Problem 2. Let $\mathcal{M} = \{\sigma_{k-1}^i\}_{i \in [L]} \subset \mathcal{K}_n$ be a subset of L distinct $(k-1)$ -simplices in \mathcal{K}_n . Output a list of ordered scores $\{s_{*,i}^{k-1}\}_{i \in [L]}$ corresponding to such alternatives.

Given $|\tilde{\mathbf{s}}_*^{k-1}\rangle$, we can implement amplitude estimation to estimate the score assigned to each $(k-1)$ -simplex by $|\mathbf{s}_*^{k-1}\rangle$. There are many different quantum amplitude estimation algorithms, but as we are more interested in

illustrating new possible avenues for applying well-established tools from QTDA rather than aiming for optimality, we stick with a relatively simple Hadamard test.

Let \mathbf{U}_{k-1}^i be a state preparation unitary such that $\mathbf{U}_{k-1}^i |0\rangle^{\otimes n} = |\sigma_{k-1}^i\rangle$ (which by Eq. (18) is simply parallel \mathbf{X} gates on the appropriate system qubits) for $\sigma_{k-1}^i \in \mathcal{M}$ and define $\mathbf{U}_{\text{amp}}^i := (\mathbf{U}_{k-1}^i \otimes \mathbf{1}^a)^\dagger \text{QTSP}(k, \mathcal{K}_n, xg_{\varepsilon'}(x^2))(\mathbf{U}_{\text{prep}} \otimes \mathbf{1}^a)$ for some $\varepsilon' > 0$. Define a Hadamard test circuit

$$\text{HAD}(\mathbf{U}) := (\mathbf{Had} \otimes \mathbf{1}^n \otimes \mathbf{1}^a) \mathbf{cU} (\mathbf{Had} \otimes \mathbf{1}^n \otimes \mathbf{1}^a), \quad (22)$$

where \mathbf{cU} denotes a controlled application of \mathbf{U} . Then, we can estimate the rescaled amplitude $(\sqrt{n}/2\kappa_k^2) \hat{s}_{*,i}^{k-1} = \langle \sigma_{k-1}^i | p(\mathbf{B}_k/\sqrt{n}) | \mathbf{s}^k \rangle = \langle 0 |^{\otimes(n+a)} \mathbf{U}_{\text{amp}}^i |0\rangle^{\otimes(n+a)}$ by estimating $P(0) = (\langle 0 | \otimes \mathbf{1}^{n+a}) \text{HAD}(\mathbf{U}_{\text{amp}}^i) (|0\rangle |0\rangle^{n+a})$, the probability of a single shot of the Hadamard test returning the outcome 0. The amplitude estimation requires $O(\log(1/\delta)/\varepsilon_{\text{AE}})$ calls to $\text{HAD}(\mathbf{U}_{\text{amp}}^i)$ and its inverse, for some $\varepsilon_{\text{AE}} > 0$, to obtain an estimate $\hat{s}_{*,i}^{k-1}$ that is $(2\kappa_k^2/\sqrt{n})\varepsilon_{\text{AE}}$ -close to $\hat{s}_{*,i}^{k-1}$ with probability of success $1 - \delta$. This leads to

$$\begin{aligned} |s_{*,i}^{k-1} - \hat{s}_{*,i}^{k-1}| &\leq \|(\mathbf{U}_{k-1}^i)^\dagger \mathbf{B}_k | \mathbf{s}^k \rangle - \frac{2\kappa_k^2}{\sqrt{n}} p(\mathbf{B}_k/\sqrt{n}) | \mathbf{s}^k \rangle\|_2 + |\hat{s}_{*,i}^{k-1} - s_{*,i}^{k-1}| \\ &\leq \varepsilon' + (2\kappa_k^2/\sqrt{n})\varepsilon_{\text{AE}} = \varepsilon, \end{aligned}$$

by setting $\varepsilon' = \varepsilon/2$ and $\varepsilon_{\text{AE}} = \varepsilon\sqrt{n}/(4\kappa_k^2)$. We perform this amplitude estimation procedure L times, one for each $(k-1)$ -simplex in \mathcal{M} , to obtain $\{\hat{s}_{*,i}^{k-1}\}_{i \in [L]}$. Given $\varepsilon, \delta > 0$, the above application requires $O(n)$ qubits and $O(L\kappa_k^2 \log(L/\delta)/(\sqrt{n}\varepsilon))$ calls to each of $\text{QTSP}(k, \mathcal{K}_n, xg_{\varepsilon/2}(x))$, \mathbf{U}_{prep} , and \mathbf{U}_{k-1}^i to obtain an ε -approximation to each of the L scores with probability $1 - \delta$ (by the union bound over all L procedures). The last step is then to order the scores to create a relative ranking of the elements in \mathcal{M} .

This is only a heuristic because, given some data \mathbf{s}^k , there is no clear way to choose ε a priori in order to guarantee that the relative ranking of \mathcal{M} obtained by the above procedure is the same as the relative ranking of these simplices according to \mathbf{s}_*^{k-1} . If a pair of amplitudes in $|\mathbf{s}_*^{k-1}\rangle$ corresponding to basis states in \mathcal{M} differ by less than 2ε , these two basis states may be out of order in the relative ranking. For example, suppose the amplitudes of $|\mathbf{s}^k\rangle$ are given by the sequence $(\frac{3}{\sqrt{n_{k-1}}}, \frac{2}{\sqrt{n_{k-1}}}, \frac{1}{\sqrt{n_{k-1}}}, \dots)$, and the aim is to relatively rank the first three alternatives. If $n_{k-1} \approx \binom{n}{k}$, then $\varepsilon = O(\binom{n}{k}^{-1/2})$ is needed in order to deduce anything meaningful from the output. For this reason this application will not achieve a large (exponential), general speedup over the classical computation, even if it does well in some cases.

VI. APPLICATION 3: FINDING A GOOD ALTERNATIVE (EXTENDED)

Problem 3. Given $|\mathbf{s}^k\rangle$, with high probability output an ordered list of alternatives $\{\sigma_{k-1}^i\}$ according to $\{\hat{s}_{*,i}^{k-1}\}$ that are ε -close to their scores $\{s_{*,i}^{k-1}\}$.

We tackle this problem using ε - ℓ_∞ -norm tomography as described in [53]. We present two of their theorems and discuss their applicability to quantum k -HodgeRank.

Theorem 2 (Corollary 17, Proposition 19 [53]). *Let $\varepsilon, \delta \in (0, 1)$ and let $|\psi\rangle = \sum_{j \in [d]} \alpha_j |j\rangle$ be a quantum state with $\alpha_j \in \mathbb{C}$. Then $O(\log(d/\delta)/\varepsilon^2)$ applications (in parallel) of a controlled state-preparation unitary for $|\psi\rangle$ suffice to compute an ε - ℓ_q -norm estimate $\tilde{\alpha}$ of α with success probability at least $1 - \delta$. On the other hand, if we only wish to learn $\tilde{\alpha}$ up to a global phase, it is sufficient to have $O(\log(d) \log(d/\delta)/\varepsilon^2)$ copies of $|\psi\rangle$, with the ability to perform unitary operations on each copy before measurement.*

We can apply these results with the unitary $\mathbf{U}_\varepsilon = \text{QTSP}(k, \mathcal{K}_n, xg_\varepsilon(x^2))(\mathbf{U}_{\text{prep}} \otimes \mathbf{1}^a)$ which prepares the state described in Eq. (20), which plays the role of $|\psi\rangle$. The dimension of the vector α , i.e., the amplitudes of the state $\mathbf{U}_\varepsilon |0\rangle^{\otimes(n+a)}$, is 2^{n+a} , where $a = O(n)$ is the number of ancilla qubits used. Thus, in the language of Theorem 2, $d = 2^{O(n)}$. Eqs. (19) and (21) together imply that

$$\left| \langle x | (\mathbf{B}_k \mathbf{B}_k^\dagger)^\dagger \mathbf{B}_k | \mathbf{s}^k \rangle - \frac{2\kappa_k^2}{\sqrt{n}} \langle x | p(\mathbf{B}_k/\sqrt{n}) | \mathbf{s}^k \rangle \right| \leq \varepsilon.$$

Setting $|x\rangle = |\sigma_{k-1}^i\rangle$ implies that $|\tilde{s}_{*,i}^{k-1} - s_{*,i}^{k-1}| \leq \varepsilon$ for all $i \in [n_{k-1}]$. Now suppose we have a classical representation of $|\hat{\mathbf{s}}_*^{k-1}\rangle$, an ε' - ℓ_∞ norm approximation to $|\tilde{\mathbf{s}}_*^{k-1}\rangle$, where $\varepsilon' = \frac{\varepsilon\sqrt{n}}{2\kappa_k}$. Then for each $i \in [n_{k-1}]$,

$$|\hat{s}_{*,i}^{k-1} - s_{*,i}^{k-1}| \leq |\hat{s}_{*,i}^{k-1} - \tilde{s}_{*,i}^{k-1}| + |\tilde{s}_{*,i}^{k-1} - s_{*,i}^{k-1}| \leq 2\varepsilon.$$

Applying Theorem 2 with $d = 2^{O(n)}$ and $\delta = 2^{-n}$, it follows that $O(\kappa_k^4 \varepsilon^{-2})$ parallel, controlled applications of \mathbf{U}_ε (i.e., of $\text{QTSP}(k, \mathcal{K}_n, xg_\varepsilon(x^2))$ and \mathbf{U}_{prep}) are required to learn $|\hat{\mathbf{s}}_*^{k-1}\rangle$ with probability $1 - 2^{-n}$, or $O(\kappa_k^4 n \varepsilon^{-2})$ applications \mathbf{U}_ε are required to learn $|\hat{\mathbf{s}}_*^{k-1}\rangle$ up to a global phase with probability $1 - 2^{-n}$.

Knowing the value of \mathbf{s}_*^{k-1} up to a global phase amounts to knowing the global order of alternatives but not knowing whether it is ranked best-to-worst or worst-to-best. In many cases, this would be possible to determine at a glance, by simply comparing the two extremes manually. In this case, one could get away with only using copies of $|\mathbf{s}_*^{k-1}\rangle$, rather than conditional applications of $\text{QTSP}(k, \mathcal{K}_n, xg_\varepsilon(x^2))$ and \mathbf{U}_{prep} . However, due to the concrete implementation of $\text{QTSP}(k, \mathcal{K}_n, xg_\varepsilon(x^2))$, this might not offer a huge advantage unless controlled access to \mathbf{U}_{prep} is unavailable.

This method for determining a good alternative is only a heuristic for similar reasons that were discussed in Appendix V: there is no way to determine an appropriate choice of ε , and there are states where ε will have to be exponentially small in k to draw meaningful conclusions from this procedure. If there was some guarantee that the scores of the alternatives all differ by at least some $\varepsilon > 0$ that does not vanish exponentially, then one can recover the exact ranking according to k -HodgeRank efficiently (provided the standard assumptions about κ_k being small). However, this is not a reasonable assumption in general. A more relaxed assumption may be that if a small set of alternatives (k -simplices) have much higher scores than the rest, classifying whether alternatives lie in this set or not may be efficient.